AD-A264 101

(2)

REPORT DOCUMENTATION PAGE

DTIC ELECTE MAY 13 1993 S C D

1a. SECURITY CLASSIFICATION: Unclassified	1b. RESTRICTIVE MARKINGS
2a. SECURITY CLASSIFICATION AUTHORITY	3. DISTRIBUTION/AVAILABILITY OF REPORT: Approved for public release; distribution unlimited.
2b. DECLASSIFICATION/DOWNGRADING SCHEDULE	
4. PERFORMING ORGANIZATION REPORT NUMBER(S)	5. MONITORING ORGANIZATION REPORT NUMBER(S)
6a. NAME OF PERFORMING ORGANIZATION: Saint Louis University; 6b. OFFICE SYMBOL (If applicable)	7a. NAME OF MONITORING ORGANIZATION: Defense Advanced Research Projects Agency
6c. ADDRESS (City, State and ZIP Code): 221 N. Grand Blvd. St. Louis, MO 63103	7b. ADDRESS (City, State and ZIP Code): 3701 N. Fairfax Drive Arlington, VA 22203-1714
8a. NAME OF FUNDING/SPONSORING ORGANIZATION Defense Advanced Research Projects Agency; 8b. OFFICE SYMBOL (If applicable): NMRO	9. PROCUREMENT INSTRUMENT IDENTIFICATION NUMBER: FY3592-91-10651
8c. ADDRESS (City, State and ZIP Code): 3701 N. Fairfax Drive Arlington, VA 22203-1714	10. SOURCE OF FUNDING NOS. — PROGRAM ELEMENT NO. / PROJECT NO. / TASK NO. / WORK UNIT NO.
11. TITLE (Include Security Classification): Attenuation & Source Studies in Northern Eurasia (unclassified)	
12. PERSONAL AUTHOR(S): J.K. Xie and B.J. Mitchell	
13a. TYPE OF REPORT: Semi-Ann. Technical; 13b. TIME COVERED: FROM 7/9/92 TO 1/8/93; 14. DATE OF REPORT (Yr., Mo., Day): 93 April 28; 15. PAGE COUNT: 32	
16. SUPPLEMENTARY NOTATION	
17. COSATI CODES — FIELD / GROUP / SUB. GR.; 18. SUBJECT TERMS (Continue on reverse if necessary and identify by block number): Seismology, Attenuation, Lg, Surface waves	

19. ABSTRACT (Continue on reverse if necessary and identify by block number)

A non-linear method is developed for the simultaneous inversion of Lg source spectra and path Q. The method is applicable to both earthquakes and explosions. The unknowns are the source corner frequency and seismic moment, as well as Lg Q_o and η values (Lg Q at 1 Hz and its power-law frequency dependence) along the paths to the recording stations. The inverse algorithm determines different Q_o and η values for each of the several paths, it is event-based, and it is suitable for real-time processing. The algorithm is further characterized by an exhaustive, non-linear search for source parameters and linear searches for Q_o and η values. The search process is implemented in successive, increasingly refined steps, designed to accelerate the computation. With these characteristics, the inverse algorithm requires neither a starting model, nor a priori information on the source and Q; it thus avoids convergence to local minima, and is fast enough to be mini-computer based.

(continued)

20. DISTRIBUTION/AVAILABILITY OF ABSTRACT: UNCLASSIFIED/UNLIMITED ☒ SAME AS RPT. ☐ OTIC USERS ☐	21. ABSTRACT SECURITY CLASSIFICATION
22a. NAME OF RESPONSIBLE INDIVIDUAL: Dr. Alan Ryall	22b. TELEPHONE NUMBER (Include Area Code): (703) 696-2245; 22c. OFFICE SYMBOL

DD FORM 1473, 83 APR EDITION OF 1 JAN 73 IS OBSOLETE.

SECURITY CLASSIFICATION OF THIS PAGE

19. Abstract (continued)

The method is applied to three underground nuclear explosions in eastern Kazakhstan. The resulting seismic moment (M_o) and corner frequency (F_c) for the largest (JVE) event are 1.3 (±0.1) x 10^{23} dyne-cm and 0.56 (±0.02) Hz, respectively. These values are consistent with previous estimates using other methods and phases, as well as the soruce scaling relationships developed for NTS explosions. Based on the same scaling relationships, the M_o values obtained for the smaller events in this study suggest seismic yields that are consistent, within reasonable uncertainties, with those predicted by using the ISC m_b values and an m_b-yield scaling relationship. The path-averaged apparent Q_o and η values agree with previous estimates in roughly the same area, but the values from individual paths can vary significantly. The apparent Q_o values are higher than 750 in two northeasterly directions, and are between 475 and 591 to three other directions. These values correlate with the regional tectonic features. These values also agree, within the uncertainties, with estimates based on a tomographic Lg coda Q_o map by Xie and Mitchell (1991).

TABLE OF CONTENTS

CONTRIBUTING SCIENTISTS

J.K. Xie	Assistant Research Professor of Geophysics
B.J. Mitchell	Reinert Professor of Geophysics

PUBLICATIONS

Xie, J., Simultaneous inversion for source spectrum and path Q using Lg with application to three Semipalatinsk explosions, *Bull. Seism. Soc. Am.*, in press, 1993.

TECHNICAL SUMMARY

A non-linear method is developed for the simultaneous inversion of Lg source spectra and path Q. The method is applicable to both earthquakes and explosions. The unknowns are the source corner frequency and seismic moment, as well as Lg Q_o and η values (Lg Q at 1 Hz and its power-law frequency dependence) along paths to the recording stations. The inverse algorithm determines different Q_o and η values for each of the several paths, it is event-based, and it is suitable for real-time processing. The algorithm is further characterized by an exhaustive, non-linear search for source parameters and linear searches for Q_o and η values. The search process is implemented in successive, increasingly refined steps, designed to accelerate the computation. With these characteristics, the inverse algorithm requires neither a starting model, nor *a priori* information on the source and Q; it thus avoids convergence to local minima, and is fast enough to be mini-computer based.

The method is applied to three underground nuclear explosions in eastern Kazakhstan. The resulting seismic moment (M_o) and corner frequency (f_c) for the largest (JVE) event are 1.3 ($\pm$ 0.1) x 10^{23} dyne-cm and 0.56 ($\pm$ 0.02) Hz, respectively. These values are consistent with previous estimates using other methods and phases, as well as the source scaling relationships developed for NTS explosions. Based on the same scaling relationships, the M_o values obtained for the smaller events in this study suggest seismic yields that are consistent, within reasonable uncertainties, with those predicted by using the ISC m_b values with an m_b-yield scaling relationship. The path-averaged apparent Q_o and η values agree with previous estimates in roughly the same area, but the values from indivi-

dual paths can vary significantly. The apparent Q_o values are higher than 750 in two northeasterly directions, and are between 475 and 591 to three other directions. These values correlate with the regional tectonic features. These values also agree, within the uncertainties, with estimates based on a tomographic Lg coda Q_o map by Xie and Mitchell (1991).

Simultaneous Inversion for Source Spectrum and Path Q Using Lg with Application to Three Semipalatinsk Explosions

ABSTRACT

A non-linear method is developed for the simultaneous inversion of Lg source spectra and path Q. The method is applicable to both earthquakes and explosions. The unknowns are the source corner frequency and seismic moment, as well as Lg Q_0 and η values (Lg Q at 1 Hz and its power-law frequency dependence) along paths to the recording stations. The inverse algorithm determines different Q_0 and η values for each of the several paths, it is event-based, and it is suitable for real-time processing. The algorithm is further characterized by an exhaustive, non-linear search for source parameters and linear searches for Q_0 and η values. The search process is implemented in successive, increasingly refined steps, designed to accelerate the computation. With these characteristics, the inverse algorithm requires neither a starting model, nor *a priori* information on the source and Q; it thus avoids convergence to local minima, and is fast enough to be mini-computer based.

The method is applied to three underground nuclear explosions in eastern Kazakhstan. The resulting seismic moment (M_0) and corner frequency (f_c) for the largest (JVE) event are 1.3 ($\pm$ 0.1) $\times$ 10^{23} dyne-cm and 0.56 ($\pm$ 0.02) Hz, respectively. These values are consistent with previous estimates using other methods and phases, as well as the source scaling relationships developed for NTS explosions. Based on the same scaling relationships, the M_0 values

obtained for the smaller events in this study suggest seismic yields that are consistent, within reasonable uncertainties, with those predicted by using the ISC m_b values and an m_b-yield scaling relationship. The path-averaged apparent Q_0 and η values agree with previous estimates in roughly the same area, but the values from individual paths can vary significantly. The apparent Q_0 values are higher than 750 in two northeasterly directions, and are between 475 and 591 to three other directions. These values correlate with the regional tectonic features. These values also agree, within the uncertainties, with estimates based on a tomographic Lg coda Q_0 map by Xie and Mitchell (1991).

Abbreviated title: Simultaneous Lg Spectral Inversion

Keywords: Non-linear optimization, Lg, Source Spectra, Q, Nuclear Explosions

1 INTRODUCTION

The seismic Lg wave train is typically the most prominent phase on short-period records observed in stable continental areas. It can be successfully modeled as a sum of higher-mode surface waves (Knopoff *et al.*, 1973), or a sum of super-critically reflected waves in the crust (Bouchon, 1982). Because Lg is so often such a prominent phase and because of its stable amplitudes, it has been used to measure sizes of seismic sources *via* a magnitude scale, m_{bLg} (Nuttli, 1973). The methodology employed in developing the m_{bLg} scale consisted of simultaneous determination of source sizes and path attenuation using time-domain data. This methodology was later extended to digital data in the spectral domain (Street *et al.*, 1975; Campillo *et al.*, 1985; Sereno *et al.*, 1988). The outcome of these studies, in terms of source characteristics and path attenuation, have provided some of the most robust estimates of sizes of the intra-plate earthquakes (Nuttli, 1973, Chow *et al.*, 1980, Alexander, 1985) and of underground nuclear explosions (Nuttli, 1986a, 1986b, 1988; Henson *et al.*, 1990; Jih, 1992). Lg attenuation has also been found to correlate with the tectonic/structural environments (*eg.*, Mitchell, 1981; Kennett *et al.*, 1985; Campillo, 1987).

Most previous simultaneous spectral inversions of source-to-Lg radiation and path Q_{Lg} have been conducted under the assumption of a constant Q model which is invariant over a large area covered by paths to all stations used in the study. In addition they were based on large data sets, typically narrow-band, collected from dense networks (*eg.*, Street *et al.*, 1975; Sereno *et al.*, 1988). Campillo *et al.* (1985) and Campillo (1987) separately measured the path-averaged Q_{Lg}, source-to-Lg radiations, and path-variable Q_{Lg} in central France using a dense seismic network. The result indicates that Q_{Lg} is highly variable within an area whose dimension is less than a few hundred km. Time domain measurement of m_{bLg} of underground nuclear explosions (Nuttli, 1986a,b, 1988; Jih, 1992) also required significant variations in Q_{Lg} among paths with lengths of a few hundred to a few thousand km.

With the deployment of modern broad-band, high dynamic range, digital seismic stations, such as the GDSN, IRIS, GEOSCOPE and CDSN stations on major continents, high quality data has become available for real time, event-based processing. This data should permit simultaneous determinations of source-to-Lg radiation and path-variable Q_{Lg} values without *a priori* knowledge on either source or Q values. In this paper, I will present a non-linear spectral method for such an inversion, and will apply it to Lg from three underground nuclear explosions in eastern Kazakhstan recorded by broad-band IRIS and CDSN stations. These applications simultaneously provide, for the first time, source spectral parameters and path-variable Q parameters. These will be compared with *a priori* knowledge, including available previous estimates of the yield of the explosions using different methods and phases, various source scaling relationships for underground explosions, and a tomographic map of Lg coda Q (Xie and Mitchell, 1991). It will be shown that the results of the applications, while requiring no *a priori* knowledge of source parameters or Q, are generally highly consistent with available *a priori* knowledge, thus demonstrating the reliability and the power of the inverse algorithm.

2. STOCHASTIC MODELING OF Lg

Street *et al.* (1975) were the first to empirically relate the Lg ground motion spectra to source spectra. Subsequent developments have incorporated the effects of finite Q (Herrmann and Kijko, 1983; Campillo *et al.*, 1985), and the stochastic nature of Lg (Xie and Nuttli, 1988; Ou and Herrmann, 1990; Xie and Mitchell, 1990) into the formulation. The formulation adopted for the inverse method of this study is that given by Xie and Nuttli (1988) and Xie and Mitchell (1990) and is expressed as

$$A_i^{Lg}(f) = S(f,\theta_i)G(\Delta_i)\exp\left[-\frac{\pi f \tau_i}{Q_i(f)}\right]X_i(f)r_i(f) \quad , \tag{1}$$

where f is frequency, $A_i^{Lg}(f)$ is the Lg displacement spectrum at the ith station, θ_i, Δ_i, τ_i and $Q_i(f)$ are the azimuth, distance, mean Lg travel time and Lg quality factor from the source to the ith station. $S(f,\theta_i)$ is the source-to-Lg spectral radiation in the direction of θ_i, or "Lg source spectrum". $G(\Delta_i)$ is the geometrical spreading factor and typically has the form

$$G(\Delta_i) = (\Delta_0\Delta_i)^{-1/2} \tag{2}$$

where Δ_0 is a reference distance. Street *et al.* (1975) and Herrmann and Kijko (1983) used a Δ_0 of 100 km and the same will be used in this study. The reason for this value is discussed in a later section. $X_i(f)$ and $r_i(f)$ in equation (1) are, respectively, the site response and the randomness due to propagation. In a laterally homogeneous medium, r_i mainly represents the random effects of multiple ray (or mode) arrivals comprising Lg, whereas in a laterally inhomogeneous medium it also represents the effects of 3D heterogeneity.

For earthquake sources, $S(f,\theta_i)$ can be represented by the omega-square model (Street *et al.*, 1975):

$$S^{eq}(f,\theta_i) = \frac{M_0 R(\theta_i)}{4\pi\rho v_s^3}\,\frac{1}{1+f^2/f_c^2} \quad , \tag{3}$$

where M_0 and f_c are the seismic moment and corner frequency of the source, ρ and v_s are average density and shear wave velocity in the crust, with typical values of 2.7 g/cm^3 and 3.5 km/s, respectively. $R(\theta_i)$ is a combination of radiation pattern and focusing/defocusing

effects in 3D media. For explosive sources, Sereno *et al.* (1988) proposed a simplified Mueller-Murphy model:

$$S^{exp}(f,\theta_i) = \frac{M_0 R(\theta_i)}{4\pi\rho v_s^3} \frac{1}{\left[1+(1-2\beta)f^2/f_c^2+\beta^2 f^4/f_c^4\right]^{1/2}} , \tag{4}$$

where we have assumed the explosion efficiency coefficient (κ in equation (7) of Sereno *et al.*, 1988) to be unity. β quantifies the overshoot effect and is defined by Mueller and Murphy (1971):

$$\beta = \frac{v_p^2}{4v_s^2} \Big|_{source} , \tag{5}$$

where " $\Big|_{source}$ " denotes quantities evaluated in the source zone.

Simultaneously inverting for f_c, M_0, $Q_i(f)$, $R(\theta_i)$ and $X_i(f)$ is normally not practical due to the trade-offs of $Q_i(f)$, $R(\theta_i)$ and $X_i(f)$. We therefore make a simplification by assuming

$$R(\theta_i)\exp\left(-\frac{\pi f \tau_i}{Q_i(f)}\right)X_i(f) = \exp\left(-\frac{\pi f \tau_i}{Q'_i(f)}\right) , \tag{6}$$

where $Q'_i(f)$ is apparent Lg Q and is assumed to have a power-law frequency dependence

$$Q'_i(f) = Q'_{0i} f^{\eta'_i} \tag{7}$$

where Q'_{0i} and η'_i are apparent Lg Q to the ith station at 1Hz and its power-law frequency dependence, respectively.

Substituting equations (2), (6) and (7) into (1), we obtain

$$A_i^{Lg}(f) = \frac{S(f)}{\sqrt{\Delta_0 \Delta_i}} \exp\left(-\frac{\pi f^{1-\eta'_i}\tau_i}{Q'_{0i}(f)}\right) r_i(f) \tag{8}$$

where $S(f)$ is given by

$$S^{eq}(f) = \frac{M_0}{4\pi\rho v_s^3} \frac{1}{1+f^2/f_c^2} \tag{9}$$

for earthquakes, and

$$S^{exp}(f) = \frac{M_0}{4\pi\rho v_s^3} \frac{1}{\left[1+(1-2\beta)f^2/f_c^2+\beta^2 f^4/f_c^4\right]^{1/2}} \tag{10}$$

for explosions. Q'_{0i} and η'_i in equations (6) through (8) will be affected not only by the Lg quality factor, but also by (i) source radiation pattern, (ii) focusing/defocusing and (iii) station site effects. The multiple higher modes comprising the Lg phase have radiation patterns which might differ from one another, but the gross Lg variation pattern is expected to be moderate (Alexander, 1985); this is particularly true for explosive sources which can be largely represented by isotropic moment tensors. The station site effect on Lg is expected to be minimal for modern broad-band stations, since they are usually installed on hard-rock sites, often in tunnels or caves. Focusing/defocusing, on the other hand, is more difficult to avoid and may produce apparent Lg Q values which differ systematically from values which would be produced by intrinsic anelasticity or by random scattering.

3. INVERSE METHOD

We assume that we have a number of stations, N, recording Lg from a single source, and that for the ith station, a number, $J(i)$, of Lg spectral estimates are available. As with previous spectral inversions for path-invariant Q (Campillo *et al.*, 1985; Sereno *et al.*, 1988), we introduce a residual square as

$$Res^2 = \sum_{i=1}^{i=N} \sum_{j=1}^{j=J(i)} \epsilon_{ij}^2 \quad , \tag{11}$$

where ϵ_{ij} is defined as

$$\epsilon_{ij} = \ln\left[4\pi\rho v_s^3 G^{-1}(\Delta_i) A_i(f_j)\right] - \ln\left[S(f_j)\exp\left(-\frac{\pi f_j^{1-\eta_i}\tau_i}{Q_{0i}}\right)\right] \quad . \tag{12}$$

f_j is the jth discrete frequency and $A_i(f_j)$ is the Fourier spectrum for the windowed time series containing Lg. It is different from $A_i^{Lg}(f_j)$ in that ambient noise and signals from other phases, such as S_n coda, may be present in $A_i(f_j)$. ϵ_{ij} is thus not identical to $\log(r_i(f_j))$ in equation (1). Q_{0i} and η_i are now used to denote *apparent* Q parameters (*i.e.*,

from now on the prime signs will be dropped for simplicity). All of the remaining symbols in equation (12) are the same as those defined in the last section.

We introduce a model parameter vector, $\mathbf{m}$:

$$\mathbf{m} = (M_0, f_c, Q_{01}, \eta_1, \ldots, Q_{0N}, \eta_N)^T \quad , \tag{13}$$

where the superscript "T" denotes transpose. Note that equation (13) implies that for explosive sources we assumed a known β (equation (5)). The residual defined in equation (11) and (12) is obviously a function of $\mathbf{m}$, and the inverse problem is defined so as to find an $\mathbf{m}_{min}$ in the model space such that

$$Res^2(\mathbf{m}_{min}) = \min \quad . \tag{14}$$

The inverse problem thus defined has two important characteristics:

(1) It is a highly overdetermined problem. The dimension of $\mathbf{m}$ is $2\times N + 2$, N being of the order of 10^0 to 10^1, whereas $\sum_i J(i)$ is usually in the order of 10^3 (*e.g.*, for the JVE event described in the application section of this paper, N is 12 and the $\sum_i J(i)$ is 1822).

(2) It is a non-linear problem (equation (8), assuming that $A_i(f)$ is reasonably close to $A_i^{Lg}(f)$), and therefore the residual (equation (11)) may have many local minima.

The first characteristics further rationalizes our parameterization of allowing Q_{0i} and η_i to be variable among paths. The second characteristics suggests that a linearized search for $\mathbf{m}_{min}$ will be successful only when a good knowledge on $\mathbf{m}_{min}$, and thereby a good starting model that is close to $\mathbf{m}_{min}$, is available. This can be difficult to obtain when in addition to the variables M_0 and f_c, Q_{0i} and η_i are allowed to be variable among paths. A full non-linear, exhaustive search for $\mathbf{m}_{min}$, on the other hand, will be very time-consuming. We therefore limit the non-linear search only to a small portion of $\mathbf{m}$. We partition $\mathbf{m}$ in the following way:

$$\mathbf{m}=(\mathbf{m}_s, \mathbf{m}_p)^T \quad , \tag{15}$$

where

$$\mathbf{m}_s = (M_0, f_c)^T \tag{16}$$

and

$$\mathbf{m}_p = (Q_{01}, \eta_1, \ldots, Q_{0N}, \eta_N)^T \quad . \tag{17}$$

We now introduce a quantity A'_{ij}, defined as

$$A'_{ij} = \ln\left[-\frac{1}{\pi\tau_i}\ln\left(\frac{A_i(f_j)}{S(f)G(\Delta_i)}\right)\right] \quad . \tag{18}$$

From equation (8) and assuming once again that $A_i^{LS}(f_j)$ is close to $A_i(f_j)$, we have

$$A'_{ij} = (1-\eta_i)\ln f_j - \ln\left(Q_{0i}\right) + e_{ij} \qquad , \quad i = 1, 2, 3, \ldots, I \tag{19}$$

where e_{ij} is a small residual. Generally there is no explicit relation between e_{ij} and ϵ_{ij}, although to the first order $\sum_{j=1}^{J(i)} e_{ij}^2$ is proportional to $\sum_{j=1}^{J(i)} \epsilon_{ij}^2$ for each of the i stations. Therefore once $\mathbf{m}_s$ is known, approximate values of the elements of $\mathbf{m}_p$ can be found by a linear regression using equations (18) and (19). Each linear regression involves quantities from a single, say the ith, station. A complete search for $\mathbf{m}$ can therefore be conducted using the following procedure:

(1) Take a possible combination of M_0 and f_c, and calculate $S(f)$ and A'_{ij} for each of the stations using equations (2), (9) (or (10)) and (18).

(2) For each of the stations, linearly estimate Q_{0i} and η_i using A'_{ij} and equation (19).

(3) Estimate the residual for $\mathbf{m}^T = (\mathbf{m}_s, \mathbf{m}_p)^T$, $\mathbf{m}_s$ being assumed in step (1) and $\mathbf{m}_p$ being obtained in step (2).

(4) Take other possible M_0 and f_c values, and repeat steps (1) through (3) in a loop, until all of the possible M_0 and f_c values are exhaustively searched and the corresponding residual values obtained.

(5) Find $\mathbf{m}_{min}$ based on the comparison of all residual square values.

In practice, the search for $\mathbf{m}_s$ can be accelerated by first using coarse intervals ΔM_0 and Δf_c for M_0 and f_c defined within possible ranges and calculate the residual values. The resulting residual square values (or $1 - Res^2$ values) are then displayed (*e.g.*, Section 5) for

roughly locating the $\mathbf{m}_s$ portion of $\mathbf{m}_{min}$. A refined search around this rough location, with much smaller intervals ΔM_0 and Δf_c, can then be conducted to find $\mathbf{m}_{min}$ to a realistic precision.

Once the *global minimum* $\mathbf{m}_{min}$ is obtained, the model covariance matrix, C_m, can be obtained using a linear perturbation suggested by Sereno *et al.* (1988):

$$C_m = \frac{Res^2}{N_d - N_p} \left(G^T G + \lambda I\right)^{-1} G^T G \left(G^T G + \lambda I\right)^{-1} \quad , \tag{20}$$

where $N_d = \sum_i J(i)$ is the total number of spectral estimates and N_p is the dimension of m. G is the Frechet kernel defined as

$$G_{ijk} = \frac{\partial}{\partial m_k} \ln\left(A_i(f_j)\right) \quad . \tag{21}$$

The square roots of the diagonal elements of C_m give the estimates for model standard errors. In this study, the value of the damping coefficient, λ, was set to be 0.001 times the minimum of diagonal elements of $G^T G$. In the following sections, I will present an application of the inverse method.

4. DATA

The inverse method is applied to Lg generated by three underground nuclear explosions in eastern Kazakhstan, near Semipalatinsk. Table 1 lists the event parameters. The largest event in Table 1 is a Joint Verification Experiment (JVE) event, which generated Lg signal with high signal/noise (S/N) ratios at five broad-band IRIS or CDSN stations. For the remaining two events, only three stations were triggered by the signals. The corresponding great circle paths are plotted in Fig. 1.

The windowing and processing of Lg is conducted in much the same way as that described by Xie and Mitchell (1990). In particular, the Lg wave train is isolated by a 20 percent cosine taper window with corners located around arrivals corresponding to group velocities of 3.10 km/s and 3.60 km/s. Fig. 2 shows an example of the time series containing Lg, and the window used, together with the Fourier spectra of the windowed signal and noise

prior to the P wave arrival.

Each Lg power spectrum is subtracted from that averaged for ten noise windows prior to P, and only those Lg spectral estimates yielding energy S/N ratio higher than about 2 are used for further analysis. The frequency bands, in which such desirable Lg spectral estimates are available, varies between about 0.2 to 0.35 Hz at their lower ends and between about 2 to 5 Hz at their higher ends.

5. RESULTS

The inverse method is applied to Lg spectral estimates for each event, with searches conducted exhaustively in the $\mathbf{m}_s$ subspace as described earlier. Two successive searches, the second one being refined from the first, are usually sufficient to find $\mathbf{m}_{min}$ with realistic precision (Table 1). A single search over 40 by 40 possible source parameter combinations, $\mathbf{m}_s$, takes less than a few minutes of CPU time on a SUN SPARC 1 work station. Fig. 3 displays the result of one search in a 3D view of 1 - Res^2 versus M_0 and f_c. The value of β is set at 0.75, corresponding to a Poisson medium. Forty three M_0 and thirty nine f_c values are searched, starting at 1×10^{22} dyne-cm and 0.4 Hz, with increments of 1 dyne-cm and 0.2 Hz, respectively. The M_0 and f_c values that are lower than those searched lead to negative Q values and are thus non-physical. The surface in Fig. 3 is fairly simple since the multiple variables Q_{0i} and η_i are not displayed, yet it is evident that convergence to a local extreme would occur if one uses a linearized search with a starting model located in the lower left portion (*i.e.*, a starting model with a large f_c and small M_0). When all of the unknowns are taken into account, the number of local extrema is expected to increase in a complex manner.

After numerically examining the result of the first search, a second search around $M_0 = 14 \times 10^{22}$ dyne-cm and $f_c = 0.6$ Hz is conducted. The optimized value of $\mathbf{m}_{min}$ leads to synthetic Lg spectra that are, over the entire frequency band, closest to the observed (Fig. 4).

To test the robustness of the resulting $\mathbf{m}_{min}$ to the value of β used, we also conducted inversions for all events with β values of 0.6 and 1.0, respectively. The resulting M_0 varied by less than 10% from those in Table 1, with the higher β value corresponding to lower M_0

values. The f_c values, when scaled by $\sqrt{\beta}$, varied by less than 0.01 Hz. This suggests that the results of this inversion are quite insensitive to varying β values, and that an inversion which includes β as an unknown will unlikely resolve it well.

Comparison of Source Parameters with Pre-existing Information

The simultaneous measurements of M_0 and f_c values (Table 1) are the first ever obtained using Lg from underground nuclear explosions. We may compare these with relevant pre-existing knowledge to check for consistency. Assuming that the M_0 values derived from Lg are equivalent to those from other body/surface waves, and assuming a portability of the M_0-yield relationship developed for the NTS by Denny and Johnson (1991, Fig. 8), the M_0 value for the JVE event in Table 1 corresponds to a seismic yield of (130 ± 10) kt. This agrees, within the estimated uncertainties, with the previous estimates obtained with seismic and non-seismic methods. For example, Priestley *et al.* (1990) obtained, by measuring time-domain amplitudes of Lg generated by the same JVE event, but recorded at stations different from those in this study, seismic yields of 148 kt and 118 kt based on the m_{bLg}-yield relationship of Nuttli (1986a) and that of Patton (1988), respectively. The uncertainty of these estimates should be at least 27% (Patton, 1988). Sykes and Ekstrom (1989), jointly using m_b and Ms, obtained a yield of 113 kt for the same JVE event, with an uncertainty factor of 1.28. Hydrodynamic measurements by US and Soviet scientists for the same event yielded values of 115 and 122 kt, respectively (*cf.*, Sykes and Ekstrom, 1989).

The f_c value for the JVE events in Table 1, if scaled by $\sqrt{\beta}$, is very close to the value of 0.7 Hz estimated from Pn/Pg waves by Priestley *et al.* (1990). A corner frequency of 0.7 Hz is also consistent with the moment-corner frequency relationship by Denny and Johnson (1991, Fig. 15), in which a yield of 120-140 kt, for example, corresponds to a corner frequency of 0.7-0.9 Hz.

Since Lg from the two smaller events triggered only 3 stations, with lower S/N ratios, our confidence on the parameters estimated for these events are somewhat lower. The average Q_0 value from the event of 12 November is also slightly lower than those from the other

two events, although they do agree within the uncertainties. Nevertheless, if we use the moment-yield relationship of Denny and Johnson as before, we can predict, for the two smaller events using the M_0 values in Table 1, yields of (26 ± 3) and (18 ± 2) kt, respectively. If we assume a minor uncertainty of 0.2 units for the m_b values in Table 1, and use the m_b-yield relationship by Sykes (Nuttli, 1986b), the probable yields will be between 9 and 23.7 kt, a range overlapping our predictions when the uncertainties are taken into account.

Finally, we note that the f_c values in Table 1 decrease, with increasing M_0 values, more slowly than that predicted by a scaling relationship of $M_0 \propto f_c^3$, which was used previously for explosions in Scandinavia (Sereno *et al.*, 1988). We feel that more work needs to be done on the Lg moment-corner frequency scaling for both explosions and earthquakes.

Comparison of Q_0 and η Values with Previous Information

The average Q_0 and η values in Table 1 agree with one another within the uncertainties, and agree with those by Given *et al.* (1988), Sereno (1990) and Chun *et al.* (1992), all obtained for Lg Q in roughly the same area. There are, however, significant variations of the Q_0 and η values from path to path (Fig. 1). The Q_0 values are above 750 to station OBN and ARU, 516 to HIA, 591 to WMQ, and 475 to GAR. The uncertainties in Fig. 1 range between about 10% to 20% for Q_0 values, and are taken from the maximum of the (i) uncertainty estimated using the square-root of the corresponding diagonal element in equation (20), and (ii) the standard error obtained in the linear regression (equation (19)). Even with the uncertainties thus estimated, it seems certain that the Q_0 value for the path to station GAR is lower than those for paths to OBN and ARU. These correlate with the regional tectonics since the former path passes through the Tienshan Mountains, whereas the latter paths lie within the shield-like Kazakhstanian and East European plates which have both been stable since Palaeozoic time (Li *et al.*, 1982).

Previous studies (Singh and Herrmann, 1983; Der *et al.*, 1984; Xie and Nuttli, 1988; Ryaboy, 1990; Xie and Mitchell, 1990) suggested that the Lg coda Q generally closely resembles the Q_{Lg} when determined in the same area. Xie and Mitchell (1991) obtained a tomographic

map of the laterally varying Lg coda Q in southern Eurasia. Fig. 5 is a map showing the Lg coda Q_0, adapted from Xie and Mitchell (1991). The paths used in this study are superposed on Fig. 5 for comparison. Like the Q_0 values in Fig. 1, the Lg coda Q_0 values in Fig. 5 are also subject to uncertainties of about 10% to 15%. Assuming a close resemblance between Lg coda Q and Lg Q, we can predict from Fig. 5 path-variable Q_0 values that are, taking into account the uncertainties, consistent with those in Fig. 1 for all paths. For example, based on Fig. 5, one can predict Q_0 values that are higher than about 700 to stations OBN and ARU, and an Q_0 value of about 450 to GAR. One can also predict that the Q_0 value to HAI is lower than that to WMQ. The consistency between the Lg Q_0 and Lg coda Q_0 values suggests that the focusing/defocusing effects on Lg, such as those predicted by Bostock & Kennett (1990), have not significantly affected the Lg Q values estimated in this study.

6. DISCUSSION

The results of applications of the inverse method in this study are dependent on the validity of stochastic modeling of Lg, particularly on validities of the geometrical spreading factor $G(\Delta)$ (equation (2)) and the simplified Mueller-Murphy source model (equation (10)). The resulting M_0, f_c, Q_0 and η value obtained in this study are consistent with *a priori* knowledge, and this consistency can be used to support these validities. Nevertheless, these validities deserve some further discussions for the clarity in future applications of the inverse method.

In this study we have used a $G(\Delta)$ of the form of equation (2), with a Δ_0 of 100 km. These were empirically proposed by Street *et al.* (1975) and were confirmed by the synthetics by Herrmann and Kijko (1983), conducted in a velocity model for the central U.S. I will hereafter refer to that model as model CUS. Strictly speaking, the value of Δ_0 is dependent on the detailed crustal velocity structure. For eastern Kazakhstan (EK), results from both DSS and receiver function studies (*cf.* Priestley *et al.*, 1988) suggest crustal velocity models which differ from model CUS. The differences include that (i) the Moho is dipping in EK, with an average depth that is a few km greater than 40 km, the depth of the Moho in model CUS; (ii)

the average velocities in the upper crust in EK is lower than in CUS. Difference (i) tends to make Δ_0 in EK greater than that in CUS, whereas difference (ii) has an opposite tendency. Overall, we expect that a Δ_0 of 100 km used in this study should not have led to significant biases in the resulting model parameters obtained. However, in future studies it will be worthwhile to investigate whether or not a Δ_0 of 100 km and a decay rate of $\Delta^{-1/2}$ are proper for various study areas (*cf.*, Bowman and Kennett, 1991).

The source model of Mueller and Murphy (1971) which was originally proposed for close-in acceleration measurements. Sereno *et al.* (1988) were the first to adapt that model into the form of equation (10) in this paper. Various other source models have also been previously proposed for explosive sources (*cf.*, Denny and Johnson, 1991). It is possible that one of the other source models could fit the Lg spectra equally well. Moreover, there are always uncertainties in the value of β as mentioned before, and in the values of ρ and v_s (equation (10)), the average density and shear wave velocity in the crust. In future studies, the non-uniqness of the source model and uncertainties in the model parameters should be kept in mind and should be reduced using *a priori* knowledge when possible.

Another uncertainty in this study is in the estimate of noise present in the Lg window. The estimate of noise in this study is based on noise *prior* to the P arrivals. The high-frequency cut-offs in this study range between about 2 and 5 hz. At higher frequencies, a more conservative estimate of noise could be obtained using Sn coda (Shin and Herrmann, 1987).

7. CONCLUSIONS

A non-linear inverse method is developed for jointly inverting for Lg source spectra and path Q. This method has the following characteristics:

(1) It allows path Q_0 and η values to be variable among paths.

(2) It is an event-based, multiple station method, suitable for real-time processing with modern broad-band stations.

(3) It searches the source parameters non-linearly and Q values linearly, requiring no starting model. The results of the inversion thus does not depend on *a priori* knowledge of the source and Q.

(4) The search algorithm is implemented with successive stages of refinement, making it fast enough to be mini-computer based.

The method is applied to three underground nuclear explosions in eastern Kazakhstan, near Semipalatinsk. The resulting seismic moment and corner frequency for the largest (JVE) event are consistent with available previous estimates using other methods, and the empirical relationships developed for NTS explosions. Assuming that the seismic moments obtained from different seismic phases are equivalent and a portability of various source-scaling relationships developed for the NTS events, the Lg seismic moments obtained in this study for the two smaller events correspond to yields that are consistent, within reasonable uncertainties, with the m_b values by the ISC.

The path-averaged Q_0 values and η values obtained in this study are consistent with previous estimates (Given *et al.*, 1990; Sereno, 1990; Chun, 1992). The Q_0 values for individual paths in this study show a correlation with the regional tectonics, and agree with a previous tomographic map of Lg coda Q_0 (Xie and Mitchell, 1991).

In future applications of the inverse method to earthquake sources, azimuthal variations of the source radiation pattern might be more significant than for explosion sources. Accordingly, interpretation of the path-variable apparent Lg Q values needs to be approached with caution.

In view of the growing high-quality broad-band seismic data base, future applications of the inverse method developed in this study will likely yield source parameters for increasing numbers of intraplate earthquakes and explosions, as well as Lg Q measurements along various paths. These should provide important input to our understanding of the excitation of Lg by various types of sources, at various depths, and to our interpretation of Q in terms of the heterogeneity, composition and evolution of the continental lithosphere.

8. ACKNOWLEDGEMENTS

I owe thanks to many people from whom this work benefited. Brian Mitchell and Bob Herrmann provided very helpful, and often inspiring, discussions and much assistance. Holly Given at UCSD provided the IRIS data and instrument responses, and patiently answered numerous questions concerning the data and instrument. Tom Carter, Paul Covacs and Jerry Carter at CSS provided CDSN data and portions of the IRIS data. Brian Mitchell and Jiang-chuan Ni critically read the manuscript. Bob Herrmann and Eric Haug maintained an excellent environment for data retrieval and numerical computation at St. Louis University. This research was supported by the Defense Advanced Research Project Agency of the Department of Defense and was monitored by the Phillips Laboratory under contract F29601-91-K-DB19, and also by the National Science Foundation under Grant EAR-9105152.

REFERENCES

Alexander, S.S. (1985). Relationship among near-field, regional, and teleseismic observations of seismic source parameters, in *The VELA Program*, Ann Kerr, (*ed.*), Defense Advanced Projects Agency, 817-829.

Bostock, M.G. & B.L.N. Kennett, (1990). Effect of 3-D structure on Lg propagation patterns, *Geophys. J. Int.*, **101**, 355-365.

Bouchon, M. (1982). The complete synthesis of seismic crustal phases at regional distances, *J. Geophys. Res.*, **87**, 1735-1741.

Bowman, J.R. and B.L.N. Kennett (1991). Propagation of Lg waves in the northern Australian craton: influence of crustal velocity gradients, *Bull. Seism. Soc. Am.*, **81**, 592-610.

Campillo, M., J. Plantet and M. Bouchon (1985). Frequency-dependent attenuation in the crust beneath central France from Lg waves: data analysis and numerical modeling, *Bull Seism. Soc. Am.*, **75**, 1395-1411.

Campillo, M. (1987). Lg wave propagation in a laterally varying crust and the distribution of the apparent quality factor in central France, *J. Geophys. Res.*, **92**, 12,604-12,614.

Chow, R.A.C., J.D. Fairhead, N.B. Henderson and P.D. Marshall (1980). Magnitude and Q determinations in southern Africa using *Lg* wave amplitudes, *Geophys. J.R. Astr. Soc.*, **63**, ,735-745.

Chun, Kin-Yip, T.F. Zhu and X.R. Shih (1992). Time-domain analysis of Lg wave attenuation in Eurasia, in *Regional wave attenuation in Eurasia, Scientific Report No. 2*, DARPA/NMRO, Arlington, Virginia, 3-12.

Denny, M.D. and L.R. Johnson (1991). The explosion seismic source function: models and scaling laws reviewed, in *Explosion Source Phenomenology*, Taylor, S.R., Patton, H.J. and Richards, P.G. (Editors), American Geophysical Union Monograph 65, Washington, D.C., 1-24.

Der, Z., M.E. Marshall, A. O'Donnell and T.W. McElfresh (1984). Spatial coherence structure and attenuation the Lg phase, site effects, and interpretation of the Lg coda, *Bull. Seism. Soc. Am.*, **74**, 1125-1148.

Given, H.K., N. Tarasov, V. Zhuravlev, F. Vernon, J. Berger, and I. Nersesov (1990). High-frequency seismic observations in eastern Kazakhstan, USSR, with emphasis on chemical explosion experiments, *J. Geophys. Res.*, **95**, 295-307.

Henson, R.A., F. Rindal, and P.G. Richards, (1990). The stability of RMS Lg measurements and their potential for accurate estimation of the yields of Soviet underground nuclear explosions, *Bull. Seism. Soc. Am.*, **80**, 2106-2126.

Herrmann, R.B. and A. Kijko (1983). Modeling some empirical Lg relations, *Bull. Seism. Soc. Am.*, **56**, 157-172.

Jih, R.S. (1992). Simultaneous inversion of explosion size and path attenuation parameter with crustal phases, *Report TGAL-92-11*, Phillips Laboratory, Hanscom Air Force Base, MA.

Kennett, B.L.N. (1984). Guided wave propagation in laterally varying media-I. Theoretical development, Geophys. J., 79, 235-255.

Kennett, B.L.N. (1986). Lg waves and structural boundaries, Bull. Seism. Soc. Am., 76, 1133-1141.

Kennett, B.L.N., S. Gregerson, S. Mykkeltveit, and R. Newmark (1985). Mapping of crustal heterogeneity in the North Sea Basin via the propagation of Lg-phases, *Geophys. J. R. astr. Soc.*, 83, 299-306.

Knopoff, L., F. Schwab, and E. Kausel (1973). Interpretation of Lg, *Geophys. J. R. astr. Soc.*, 33, 389-404.

Li, C., Q. Wang, X. Liu and Y. Tang, 1982. Explanatory notes to the tectonic map of Asia, *Cartographic Publishing House*, Beijing, China, 49pp.

Mitchell, B.J. (1981). Regional variation and frequency dependence of Q_β in the crust of the United States, *Bull. Seismo. Soc. Am.*,, 71, 1531-1538.

Mueller, R.A. and J.R. Murphy, (1971). Seismic characteristics of underground nuclear explosions, Part I., Seismic spectrum scaling, *Bull. Seism. Soc. Am.*, 61, 1675-1692.

Nuttli, O.W. (1973). Seismic wave attenuation and magnitude relations for eastern North America, *J. Geophys. Res*, 78, 876-885.

Nuttli, O.W. (1986a). Yield estimates of Nevada Test Site explosions obtained from seismic Lg waves, *J. Geophys. Res.*, 91, 2737-2151.

Nuttli, O.W. (1986b). Lg magnitudes of selected East Kazakhstan underground explosions, *Bull. Seism. Soc. Am.*, 76, 1241-1251.

Nuttli, O.W. (1988). Lg magnitudes and yield estimates for underground Novaya Zemlya nuclear explosions, *Bull. Seism. Soc. Am.*, 78, 873-884.

Ou, G.B. and R.B. Herrmann (1990). A statistical model for ground motion produced by earthquakes at local and regional distances, *Bull. Seism. Soc. Am.*, *80*, 1397-1417.

Patton, H.J. (1988). Application of Nuttli's method to estimate yield of Nevada Test Site explosions recorded on Lawrence Livermore National Laboratory's digital seismic system, *Bull. Seism. Soc. Am.*, 78, 1759-1772.

Priestley, K.F., Zandt, G. & Randall, G.E., (1988). Crustal structure in eastern

Priestley, K.F., W.R. Walter, V. Martynov, and M.V. Rozhkov (1990). Regional seismic recordings of the Soviet nuclear explosion of the Joint Verification Experiment, *Geophys. Res. Lett.*, 17, 179-182.

Ryaboy, V.Z. (1990). Earth crust and upper mantle Q-structure beneath northern Eurasia, (abs), *Seismo. Res. Lett.*, 62, 32.

Sereno, T.J., S.R. Bratt and T.C. Bache (1988). Simultaneous inversion of regional wave spectra for attenuation and seismic moment in Scandinavia, *J. Geophys. Res.*, 93, 2019-2036.

Sereno, T.J., 1990. Frequency-dependent attenuation in eastern Kazakhstan and implications for seismic detection thresholds in the Soviet Union, *Bull. Seism. Soc. Am.*, 80, 2089-2105.

Shin, T.-C. and R. B. Herrmann (1987). Lg attenuation and source studies using 1982 Miramichi data, *Bull. Seism. Soc. Am.*, 77, 384-397.

Singh, S.K. and R.B. Herrmann (1983). Regionalization of crustal coda Q in the continental United States, *J. Geophys. Res.*, **88**, 527-538.

Street, R.L., R.B. Herrmann and O.W. Nuttli (1975). Spectral characteristics of the Lg wave generated by central United States earthquakes, *J. Geophys. Res.*, **41**, 51-63.

Sykes, L. and G. Ekstrom (1989). Comparison of seismic and hydrodynamic yield determinations for the Soviet Joint Verification Experiment of 1988, *Proc. Natl. Acad. Sci. USA*, **86**, 3456-3460.

Xie, J. and O.W. Nuttli (1988). Interpretation of high-frequency coda at large distances: stochastic modeling and method of inversion, *Geophys. J.*, **95**, 579-595.

Xie, J. and B.J. Mitchell (1990). Attenuation of multiphase surface waves in the Basin and Range Province, part I: Lg and Lg coda, *Geophys. J. Int.*, **102**, 121-137.

Xie, J. and B.J. Mitchell B.J. (1991). Lg coda Q across Eurasia, in *Yield and discrimination studies in stable continental regions*, B.J. Mitchell (ed). Report PL-TR-91-2286, Phillips Laboratory, Hanscom Air Force Base, MA, 77-91.

Table 1. Event and path parameters †

Event Date	Origin Time	m_b	Location	Seismic Moment (dyne.cm)	Corner Frequency	Average Q_0	Average η
Sep. 14, 88*	3H59M57.6S	6.1	49.81°N, 78.80°E	$1.3 (\pm 0.1) \times 10^{23}$	0.56 ± 0.02 hz	657 ± 129	0.31 ± 0.02
Nov. 12, 88	3H30M30.8S	5.4	50.05°N, 78.98°E	$2.6 (\pm 0.3) \times 10^{22}$	0.82 ± 0.02 hz	557 ± 94	0.48 ± 0.01
Nov. 23, 88	3H57M06.8S	5.4	49.77°N, 78.06°E	$1.8 (\pm 0.2) \times 10^{22}$	0.70 ± 0.02 hz	621 ± 127	0.49 ± 0.02

† The origin times, locations and magnitudes are from the ISC bulletin; the seismic moments, corner frequencies and path-averaged Q_0 and η values are obtained in this study with β in equation (5) set to be 0.75 (Poisson media).

* The Joint Verification Experiment (JVE) event.

Figure Captions

Fig. 1. Great circle paths from the three nuclear explosions to the IRIS/CDSN stations. Numbers near the paths are the Q_{0i} and η_i values obtained for the path, with the estimated uncertainties.

Fig. 2. (Top) Time series containing Lg from the JVE event observed at IRIS station ARU. The trace is instrument uncorrected, and starts at group velocity of 4.1 km/s, corresponding to a lapse time of 374.0 sec. The smooth curve represents a 20 percent cosine window used in the analysis. (Bottom) The instrument- uncorrected Fourier amplitude spectrum of the signal containing Lg, and the Fourier spectra from several noise windows prior to P.

Fi. 3. 1 - Res^2 versus M_0 and f_c resulting from a search over 43 M_0 values (between 8 to 50 $\times 10^{22}$ dyne-cm) and 39 f_c values (between 0.4 to 8.0 Hz), with respective intervals of 1 $\times 10^{22}$ dyne-cm and 0.2 Hz. The β value (equation (5)) is set to be 0.75. Note that the Q_{0i} and η_i values are not displayed, making the surface considerably simpler, with fewer local extrema.

Fig. 4. Synthetic Lg spectra for all of the five stations recording the JVE event, versus the observed. The spectra are normalized to source by multiplying by $4\pi\rho v_s^3 \left(\Delta_0\Delta\right)^{-1/2}$ (*ie.*, arguments of the first and second logarithms in equation (12) are the observed and synthetic spectra displayed here, respectively). The units used are (Hz) for frequency and (10^{22} dyne-cm) for amplitude. The synthetic spectra are calculated using the optimal source model parameters in Table 1, and optimal Q_{0i}, η_i parameters indicated above each panel.

Fig. 5. Tomographic map of laterally varying Lg coda Q_0 in the area under study, adapted from Xie and Mitchell (1991). The paths used in this study are superposed for comparison.

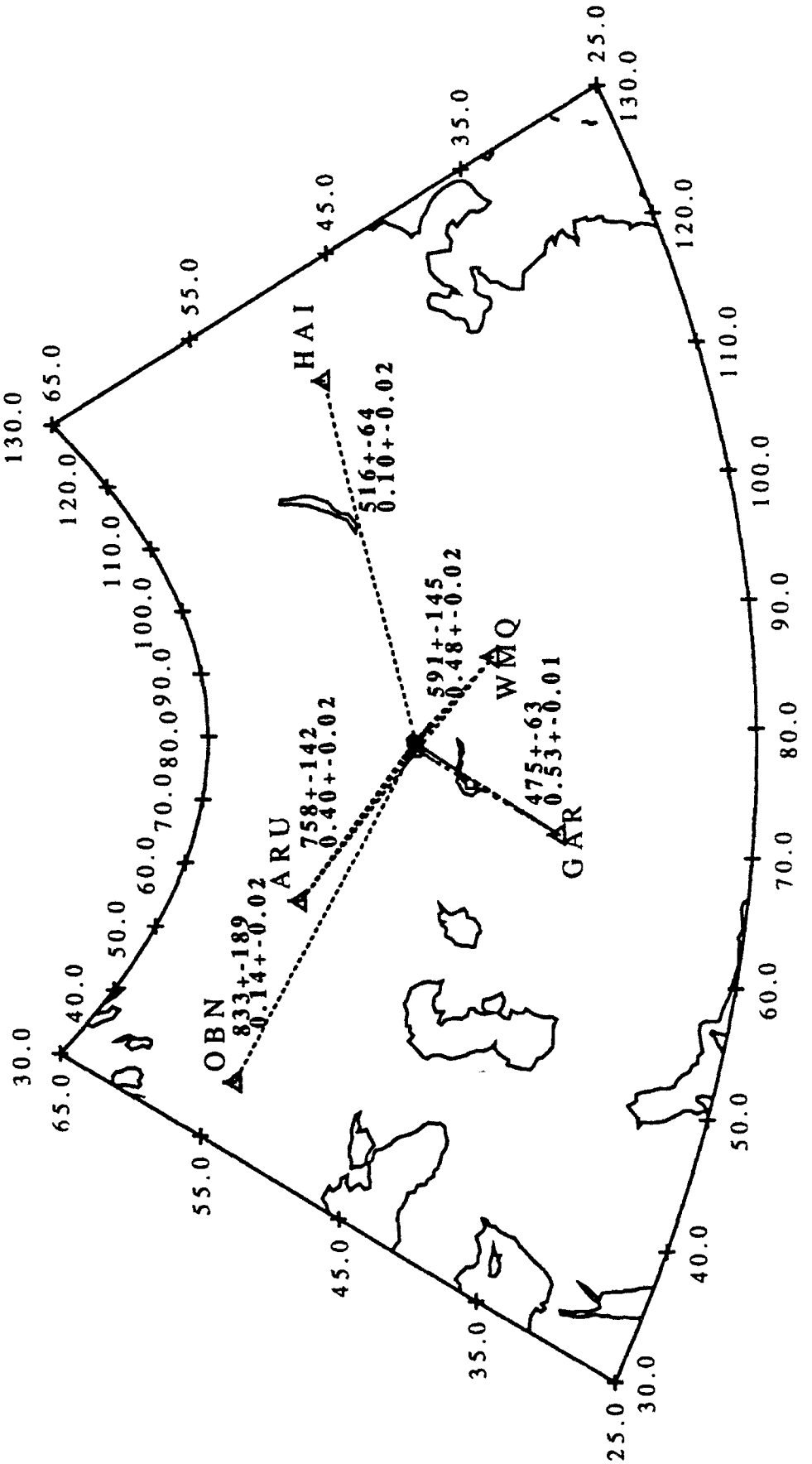
HAI
516+-64
0.10+-0.02
591+-145
0.48+-0.02
WMQ
475+-63
0.53+-0.01
GAR
758+-142
0.40+-0.02
ARU
833+-189
0.14+-0.02
OBN
130.0
120.0
110.0
100.0
90.0
80.0
70.0
60.0
50.0
40.0
30.0
65.0
55.0
45.0
35.0
25.0

Fig 1

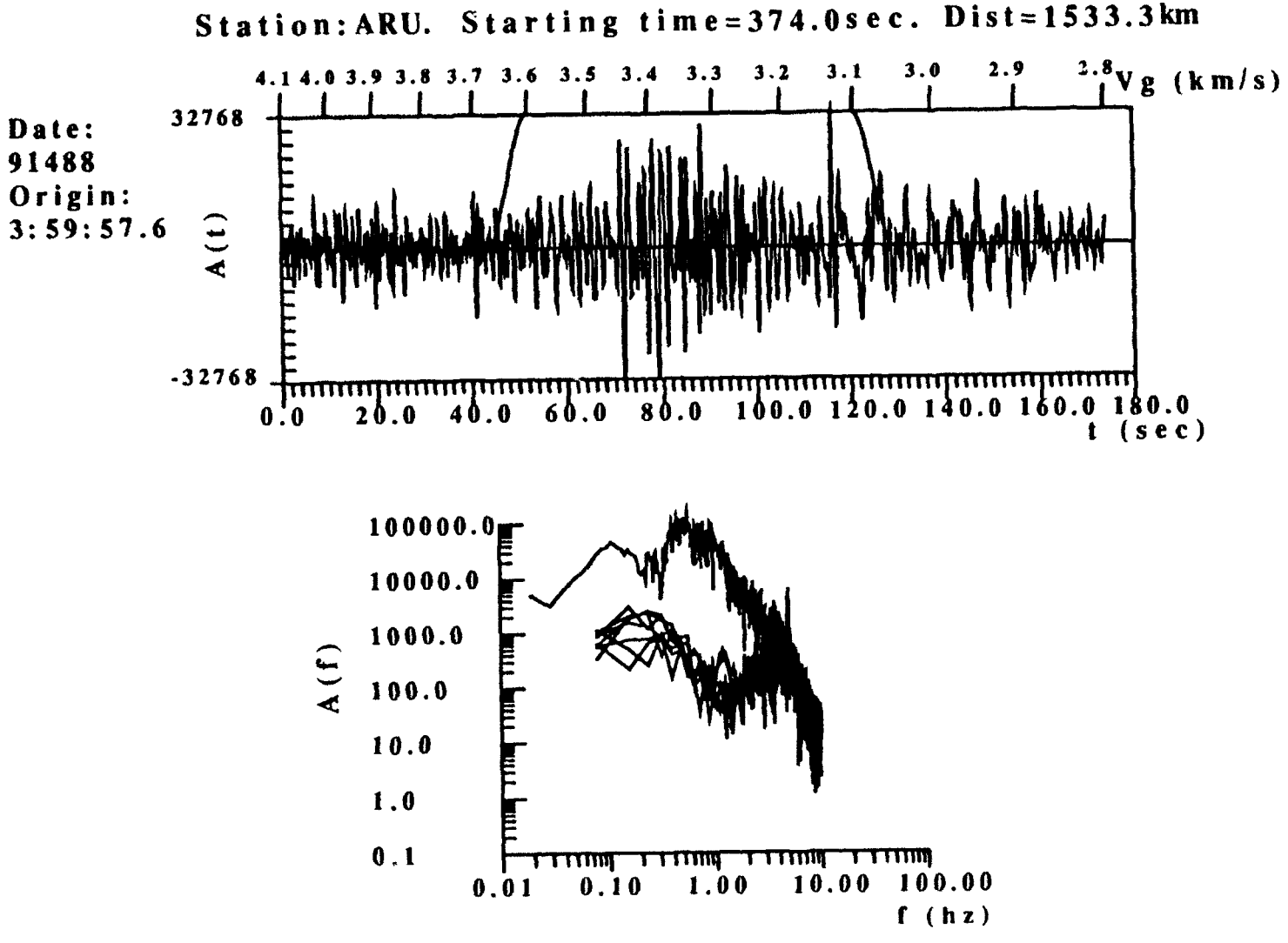
Station:ARU. Starting time=374.0sec. Dist=1533.3km
Date:
91488
Origin:
3:59:57.6
4.1 4.0 3.9 3.8 3.7 3.6 3.5 3.4 3.3 3.2 3.1 3.0 2.9 2.8 Vg (km/s)
32768
-32768
A(t)
0.0 20.0 40.0 60.0 80.0 100.0 120.0 140.0 160.0 180.0
t (sec)
100000.0
10000.0
1000.0
100.0
10.0
1.0
0.1
A(f)
0.01 0.10 1.00 10.00 100.00
f (hz)

Fig 2

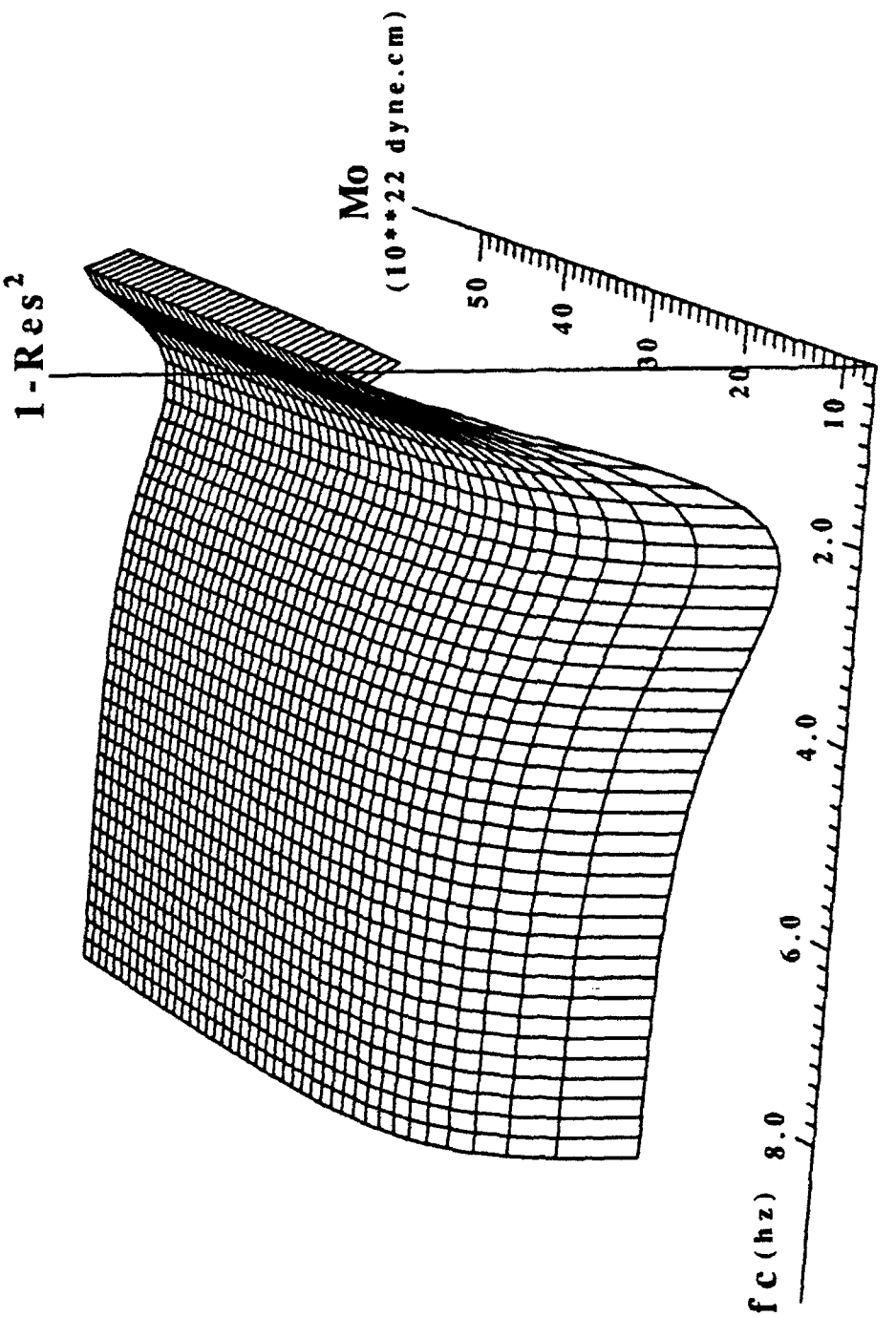

Fig 3

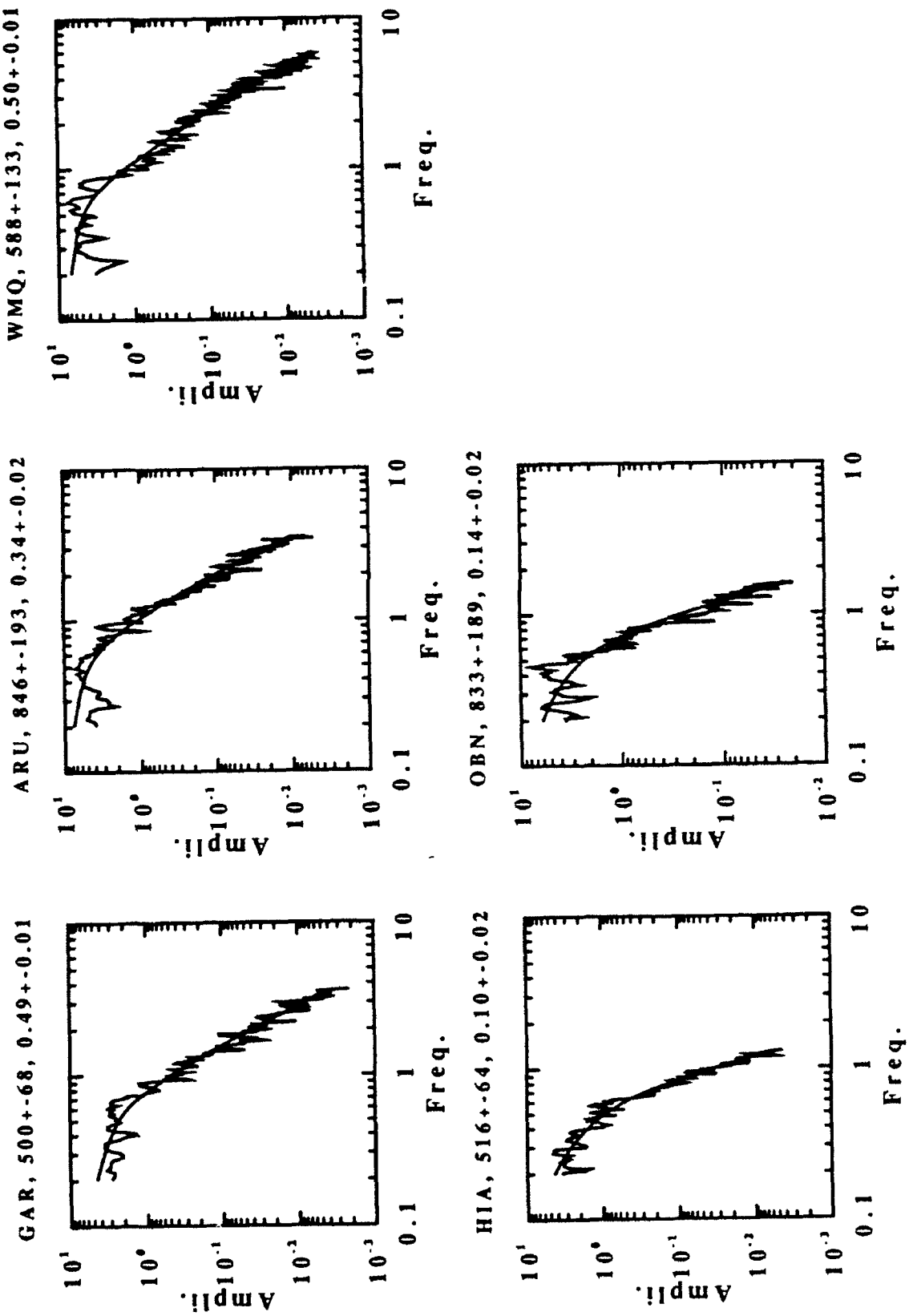
WMQ, 588+-133, 0.50+-0.01
ARU, 846+-193, 0.34+-0.02
OBN, 833+-189, 0.14+-0.02
GAR, 500+-68, 0.49+-0.01
HIA, 516+-64, 0.10+-0.02
Ampli.
Freq.
0.1
1
10

Fig 14

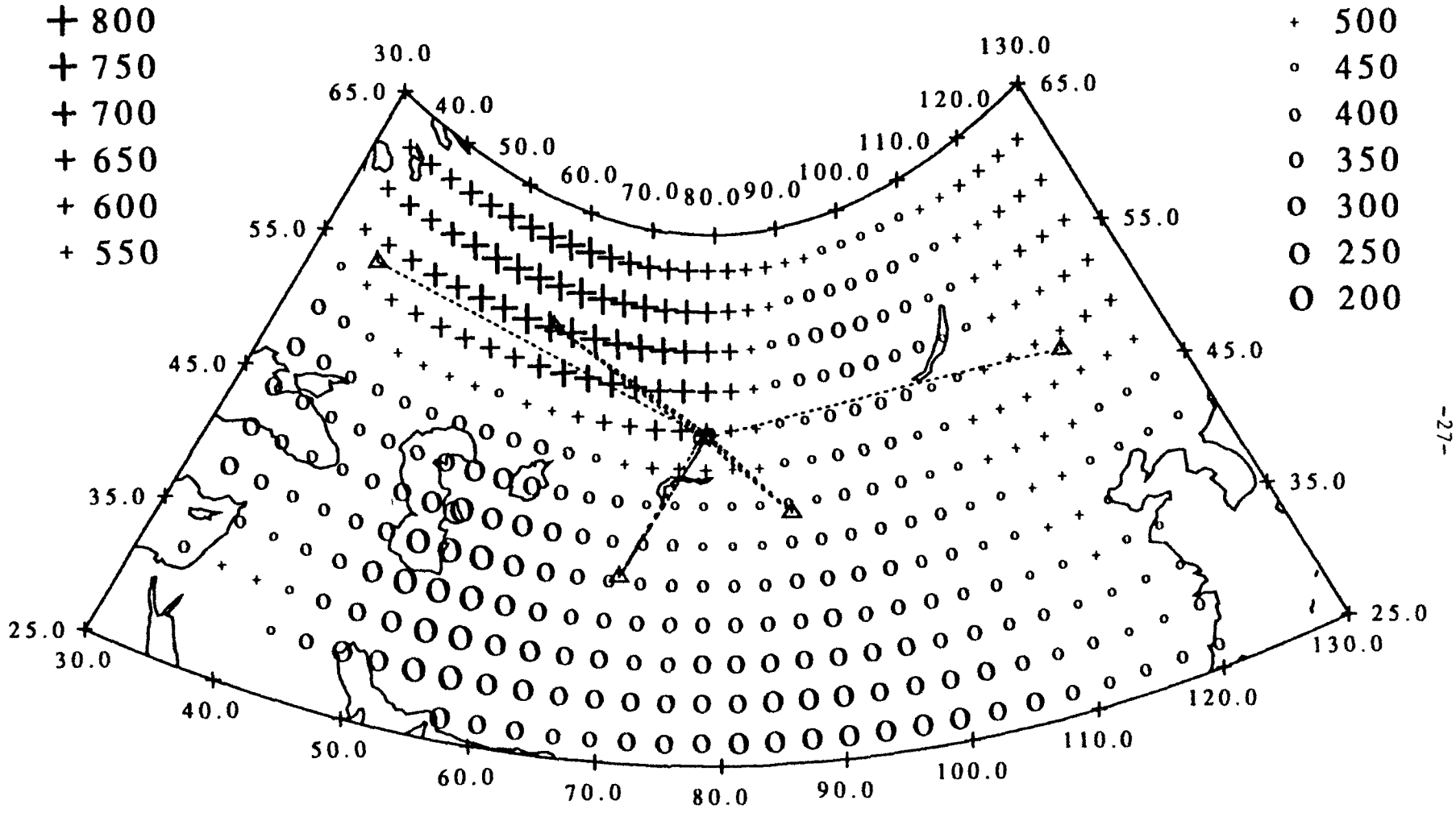
+ 800
+ 750
+ 700
+ 650
+ 600
+ 550
+ 500
o 450
o 400
o 350
o 300
O 250
O 200
30.0
65.0
40.0
50.0
60.0
70.0
80.0
90.0
100.0
110.0
120.0
130.0
55.0
45.0
35.0
25.0

Fig 5